Allyl isothiocyanate induces G_2/M arrest in human colorectal adenocarcinoma SW620 cells through down-regulation of Cdc25B and Cdc25C

WING-SZE LAU[1], TIANFENG CHEN[1,2,3] and YUM-SHING WONG[1,2]

[1]State Key Laboratory of Agrobiotechnology, and [2]Food and Nutritional Sciences Programme, Department of Biology, The Chinese University of Hong Kong, Hong Kong SAR; [3]Department of Chemistry, Jinan University, Guangdong, P.R. China

Received May 13, 2010; Accepted August 16, 2010

DOI: 10.3892/mmr.2010.363

Abstract. Allyl isothiocyanate (AITC) is a constituent of cruciferous vegetables that exhibits antitumor activity. In this study, AITC was shown to inhibit the proliferation of human metastatic colorectal adenocarcinoma SW620 cells *in vitro* by inducing cell cycle arrest at the G_2/M phase. The signaling pathway of AITC action involved the down-regulation of the pivotal Cdc25B and Cdc25C protein phosphatases in the treated cells. Quantitative real-time PCR of AITC-treated SW620 cells revealed a time-dependent down-regulation of Cdc25B and Cdc25C mRNA levels, which resulted in a decrease in the expression levels of these two proteins. Upon prolonged exposure, AITC induced caspase-mediated apoptosis in SW620 cells. The apoptotic process was evidenced by the activation of initiator caspases (-8 and -9) and effector caspases (-3 and -7), and the cleavage of poly(ADP-ribose) polymerase (PARP). The antitumor activity of AITC was further demonstrated in a SW620 xenograft *in vivo*. Taken together, the results suggest that AITC is a potential candidate for future research in chemoprevention and chemotherapy.

Introduction

Colorectal cancer is one of the most prevalent cancers, and is a leading cause of cancer-related death in developed countries (1). Numerous epidemiological studies indicate that a high intake of cruciferous vegetables, such as cabbage, broccoli and Brussels sprouts, may reduce the risk of developing the disease. It is suggested that glucosinolates present in cruciferous vegetables play a key role in this function (2-4). Glucosinolates are a class of compounds that are composed of a sulphonated moiety, a β-thioglucose and variable side-chains (5). When plant tissue is physically damaged, the glucosidic bond is cleaved by endogenous myrosinase producing various products, including isothiocyanates (ITCs), thiocyanates and nitriles (5). Upon human ingestion, the remaining glucosinolates may also be broken down by colonial bacteria (6-8). Among these breakdown products, ITCs draw most of the attention due to their antitumor activities.

Recent reports showed that several ITCs, including allyl isothiocyanate (AITC), benzyl isothiocyanate, phenylethyl isothiocyanate (PEITC) and sulforaphane (SFN), possessed inhibitory effects on the growth of human cancer cells (9-19). These inhibitory effects were associated with the induction of cell cycle arrest (10,12,16-19) and apoptosis (9-11,13-15,17,18). In these studies, it was proposed that ITC-induced cell cycle arrest was controlled by post-translational modulation of checkpoint regulatory proteins (16-19), and ITC-induced cell apoptosis was mediated by the activation of caspases and/or Bcl-2 family proteins (9,10,13-15,17). Despite these findings, the sequence of molecular events resulting in this effect has yet to be determined. In animal experiments employing potent carcinogens, treatment with ITCs suppresses the process of carcinogenic activation and inhibits tumorigenesis in the lungs (20-22). Previous studies also revealed that ITCs suppressed the growth of prostate cancer PC-3 xenografts (15,23). Tumor suppression was found to be correlated with the inhibition of cell proliferation and/or the induction of apoptosis after treatment (15,23). In this study, the chemotherapeutic potential of AITC, a major ITC, was examined in human metastatic colorectal adenocarcinoma SW620 cells *in vitro* and *in vivo*. The underlying molecular mechanism, especially at the transcriptional level of control, was investigated.

Materials and methods

Materials. AITC was purchased from International Laboratory Limited (San Bruno, CA, USA). A cell proliferation ELISA 5-bromo-2'-deoxyuridine (BrdU) colorimetric assay kit was supplied by Roche Diagnostics GmbH (Mannheim, Germany). Antibodies against β-actin, Cdc2, p-Cdc2(Thr14), p-Cdc2(Tyr15), p-Cdc25C(Ser216), Cdc25C, caspases-3, -6, -7, -8, -9 and poly(ADP-ribose) polymerase (PARP)

Correspondence to: Dr Yum-shing Wong, Department of Biology, Science Centre, The Chinese University of Hong Kong, Shatin, New Territories, Hong Kong SAR, P.R. China
E-mail: yumshingwong@cuhk.edu.hk

Key words: allyl isothiocyanate, apoptosis, G_2/M arrest, colorectal cancer

were obtained from Cell Signaling Technology (Danvers, MA, USA). Antibodies against Cdc25B and CyclinB1 were purchased from Abcam (Cambridge, MA, USA). Fetal bovine serum (FBS) was from HyClone (Logan, UT, USA). Phosphate buffered saline (PBS), penicillin-streptomycin, Leibovitz's-15 (L-15) and Dulbecco's modified Eagle's medium (DMEM) were obtained from Gibco (Rockville, MD, USA). Bovine serum albumin (BSA), dimethyl sulfoxide (DMSO), propidium iodide (PI), propylene glycol, protease inhibitor cocktail, ribonulease A (RNase A), RPMI-1640 medium and 3-(4,5-dimethylthiazol-2-yl)-2,5-diphenyltetrazolium bromide (MTT) were supplied by Sigma Chemical Co. (St. Louis, MO, USA).

Cell lines and cell cultures. Human skin fibroblast Hs68 cells and human colorectal adenocarcinoma Caco-2, COLO 201 and SW620 cells were obtained from the American Type Culture Collection (Manassas, VA, USA). Caco-2 and Hs68 cells were cultured in DMEM, whereas COLO 201 and SW620 cells were cultured in RPMI-1640 and L-15 medium, respectively. The cells were supplemented with 10% FBS and 1% penicillin (10,000 U/ml)-streptomycin (10,000 μg/ml). Caco-2, COLO 201 and Hs68 cells were regularly maintained at 37˚C in a humidified atmosphere of 95% air and 5% CO_2, whereas SW620 cells were cultured without CO_2.

Cell viability/proliferation assays. The effects of AITC on the survival and proliferation of different cell lines were determined by cell viability MTT and cell proliferation BrdU assays, as previously described (24). AITC was prepared by dilution with DMSO, with a final concentration of DMSO of 0.5% employed in the assays. An equivalent amount of DMSO was used as a control. In the MTT assay, cell viability was determined by measuring the ability of viable cells to transform a yellow tetrazolium salt (MTT) into a dark blue formazan product. In brief, cultured cells ($2.5x10^3$ to $1x10^4$ cells/well) were pre-seeded into a 96-well tissue culture plate for 24 h. Cells were then exposed to 0-150 μM AITC for varying time periods. Following incubation, 20 μl of freshly prepared MTT solution (5 mg/ml in PBS) was added to each well, and the cells were further incubated for 5 h. The culture medium was then removed and 150 μl acid-isopropanol (0.04 N HCl in isopropanol) was added to dissolve the formazan product. Absorbance was measured at 570 nm using a SpectraMax250 microplate reader (Molecular Devices, CA, USA). In addition to the MTT assay, the anti-proliferative effect of AITC was confirmed by the BrdU assay. In this assay, quantification of cell proliferation is based on the measurement of BrdU incorporation during DNA synthesis. The SW620 cells were prepared in the same way as in the MTT assay, and the procedures were performed according to the manufacturer's protocol (Roche Diagnostics GmbH).

Determination of cell cycle distribution by flow cytometry. The cell cycle distribution was analyzed by flow cytometry as previously described (24). SW620 cells ($1x10^6$) were pre-seeded into T75 tissue culture flasks for 24 h. The cells were then subjected to various AITC treatments. The treated cells were trypsinized, washed with PBS and fixed with ice-cold 70% ethanol at -20˚C overnight. The fixed cells were washed twice with PBS and once with 1% BSA in PBS, and then resuspended in DNA-binding PI solution (700 U/ml RNase A, 50.1 μg/ml PI, pH 8.0) at 4˚C overnight. After labeling with PI, the cells were analyzed with a Beckman Coulter Epics XL-MCL flow cytometer (Miami, FL, USA). Cell cycle distribution was analyzed using MutliCycle software (Phoenix Flow Systems, San Diego, CA, USA). Cells with hypodiploid DNA content were regarded as the apoptotic cell population.

Western blot analysis. AITC-treated SW620 cells were trypsinized and washed with PBS. Cell lysate was prepared by incubating the harvested cells in lysis buffer (Cell Signaling Technology) containing protease inhibitor cocktail for 50 min on ice. The clear supernatant was collected following centrifugation at 14,000 rpm for 15 min at 4˚C. The protein concentration of the lysate was determined using a bicinchoninic acid protein assay kit according to the manufacturer's protocol (Sigma Chemical Co.). Samples containing 10-60 μg proteins were resolved by SDS-polyacrylamide gel electrophoresis (4% stacking; 10% resolving) and transferred onto a nitrocellulose membrane (Amersham Life Science, Buckinghamshire, UK) (25). The membrane was first incubated with blocking buffer [1X Tris-buffered saline, 0.1% Tween-20, 5% (w/v) non-fat dry milk] for 1 h at room temperature (RT). The blot was then incubated with the desired primary antibody (1:1,000-3,000) at 4˚C overnight. After washing, the membrane was incubated with corresponding horseradish peroxidase-conjugated secondary antibodies (1:2,000) for 1 h at RT. Immunodetection was achieved using LumiGLO reagent® (Cell Signaling Technology) with the emitted light captured on X-ray film. The membranes were stripped and re-probed with β-actin to check the uniformity of the protein loading.

Quantitative real-time PCR. AITC-treated SW620 cells were trypsinized and washed with PBS. Total RNA was extracted from the harvested cells using TRI-Reagent (Molecular Research Center, Cincinnati, OH, USA) according to the manufacturer's protocol. cDNA was synthesized from total RNA by reverse transcription using Superscript™ III reverse transcriptase according to the manufacturer's protocol (Invitrogen Corp., CA, USA). Real-time PCR primers of the selected genes were chosen according to a previous study (26) and using Primer3 software (http://frodo.wi.mit.edu/cgi-bin/primer3/primer3_www.cgi) based on the sequence data obtained from the NCBI database (http://www.ncbi.nlm.nih.gov/) (Table I). Real-time PCR amplification of cDNA was carried out using the BioRad iQ™5 real-time PCR detection system (BioRad Laboratories, Hercules, CA, USA) in a 96-well PCR plate with a dome cap under the following cycling conditions: 3 min at 95˚C and 40 cycles at 95˚C for 10 sec, followed by 30 sec at 55˚C. The reaction mixture comprised 10 μl of iQ™ SYBR Green Supermix (BioRad Laboratories) and 0.4 μM each of the forward and reverse primers in a total reaction volume of 20 μl. The expression level of each gene was normalized with the housekeeping gene glyceraldehydes 3-phosphate dehydrogenase (GAPDH). Relative gene expression was calculated using the $2^{-\Delta\Delta CT}$ method (27). Simultaneously, a single sharp peak was noted in the dissociation curve for the confirmation of accuracy.

Table I. Primers used for quantitative real-time PCR.

Gene	Forward primer (5'-3')	Reverse primer (5'-3')
GAPDH	AGATCATCAGCAATGCCTCCTG	ATGGCATGGACTGTGGTCATG
Cdc25B	ACGATGGTGGCCCTATTGAC	GCAAGTTCACCGCAGTCTTG
Cdc25C	TTTTTCCAAGGTATGTGCGCTG	TGGAACTTCCCCGACAGTAAGG
CyclinB1	TCGAGCAACATACTTTGGCCA	GCAAAAAGCTCCTGCTGCAA

In vivo xenograft study. The procedures for the *in vivo* xenograft study were similar to those described in our previous study (28). Animal experimentation followed the guidelines approved by the Animal Experimentation Ethics Committee of The Chinese University of Hong Kong. Male BALB/c nude mice (nu/nu) (6-7 weeks) were supplied by the Laboratory Animal Services Centre, CUHK. The mice were housed in filtered cages and maintained under controlled laboratory conditions (22-25˚C, 12/12 h light/dark cycle) with *ad libitum* access to sterile rodent chow and water, and were acclimatized for 4 days prior to the experiment. SW620 cells ($2x10^6$ cells/site) in 0.3 ml fresh culture medium were injected subcutaneously into the back of each of 24 mice, which were then randomly divided into three groups. Starting from the day of cell inoculation, two treatment groups received intraperitoneal (i.p.) injection (3 times/week) of 5 and 10 μmol AITC, respectively. The control group received an equal volume of vehicle (0.1 ml, 8% propylene glycol in PBS, v/v). Mice were monitored regularly and their body weight was recorded periodically in order to assess their health. When a palpable tumor appeared, the tumor size was measured periodically using a caliper. Tumor volume was calculated using the equation: tumor volume (mm^3) = (length x $width^2$)/2. At the termination of the experiment, the mice were sacrificed using CO_2 asphyxiation. The tumors were removed from the animals and the tumor mass was measured.

Statistical analysis. The results are expressed as the mean ± SD of at least three independently performed experiments, unless indicated otherwise. Statistical differences between the control and treatment groups were determined using the two-tailed Student's t-test. A difference of $^{*}P<0.05$ or $^{**}P<0.01$ was considered statistically significant.

Results

AITC inhibits the growth of human colorectal adenocarcinoma cells in vitro. In a screening test on the antitumor activity of AITC, three human colorectal adenocarcinoma cell lines, namely Caco-2, COLO 201 and SW620, were found to be susceptible to AITC. As shown in Fig. 1A, after treatment with 50 μM AITC for 72 h, the survival percentage of Caco-2, COLO 201 and SW620 cells as determined by the MTT assay was 50.7, 64.6 and 42.0%, respectively. By contrast, the survival of normal human skin fibroblast Hs68 cells was not significantly affected by AITC. The dose- and time-dependent cytotoxic effect of AITC on SW620 cells is shown in Fig. 1B. The anti-proliferative activity of AITC against SW620 cells was demonstrated using the BrdU assay (Fig. 1C). Microscopic examination also revealed an apparent decrease in cell density and a change in cell morphology after AITC treatment (Fig. 1D).

AITC induces cell cycle arrest at the G_2/M phase in SW620 cells. In order to investigate the anti-proliferative effect of AITC, the cell cycle distribution of AITC-treated SW620 cells was analyzed using flow cytometry. As shown in Fig. 2, AITC modulated the progression of the cell cycle in a dose- and time-dependent manner. Accumulation of cells at the G_2/M phase, together with the concomitant diminution of cells at the G_0/G_1 phase, was observed (Fig. 2A and B). Cell cycle arrest at the G_2/M phase began 4 h after AITC treatment and reached a maximum at 24 h (Fig. 2C). Subsequently, an increase in cells arrested at the S phase was observed (Fig. 2C), which indicated that an impaired progression had occurred at the G_2/M transition.

AITC modulates the expression of regulatory proteins for G_2/M transition. In order to elucidate the underlying mechanisms of G_2/M arrest in AITC-treated SW620 cells, the expression of pivotal regulatory proteins was studied. At the G_2 checkpoint, the control of the Cdc2/CyclinB kinase complex is crucial for cells to proceed into mitosis, and is governed by the action of two phosphatases, namely Cdc25B and Cdc25C (29-31). The results indicated that AITC treatment led to the down-regulation of Cdc25B and Cdc25C proteins in a dose- and time-dependent manner (Fig. 3A and B). A marked down-regulation of Cdc25C was observed after 8 h of treatment (Fig. 3B). Simultaneously, AITC treatment caused short-term phosphorylation of Cdc25C on Ser216 (a negative regulatory site) during the first 4 h. The later down-regulation of p-Cdc25C(Ser216) may have been due to the concomitant decrease of Cdc25C in that time interval. Similarly, down-regulation of another phosphatase, Cdc25B, was also observed. Without the catalytic action of both phosphatases, the Cdc2 kinase was modulated by inhibitory phoshorylation on Thr14 and Tyr15 (Fig. 3A and B). A rapid and sustained up-regulation of p-Cdc2(Tyr15) was noted after 1 h of treatment, and another phosphorylation site on Thr14 was observed after 24 h (Fig. 3B). The up-regulation of CyclinB1 was also observed in AITC-treated SW620 cells (Fig. 3A and B).

AITC modulates the expression of regulatory genes for G_2/M transition. In order to verify whether the change in protein expression of Cdc25B and Cdc25C was related to the transcriptional level of control, the effects of AITC on the expression of related genes was investigated. The results of quantitative real-time PCR studies on the expression of

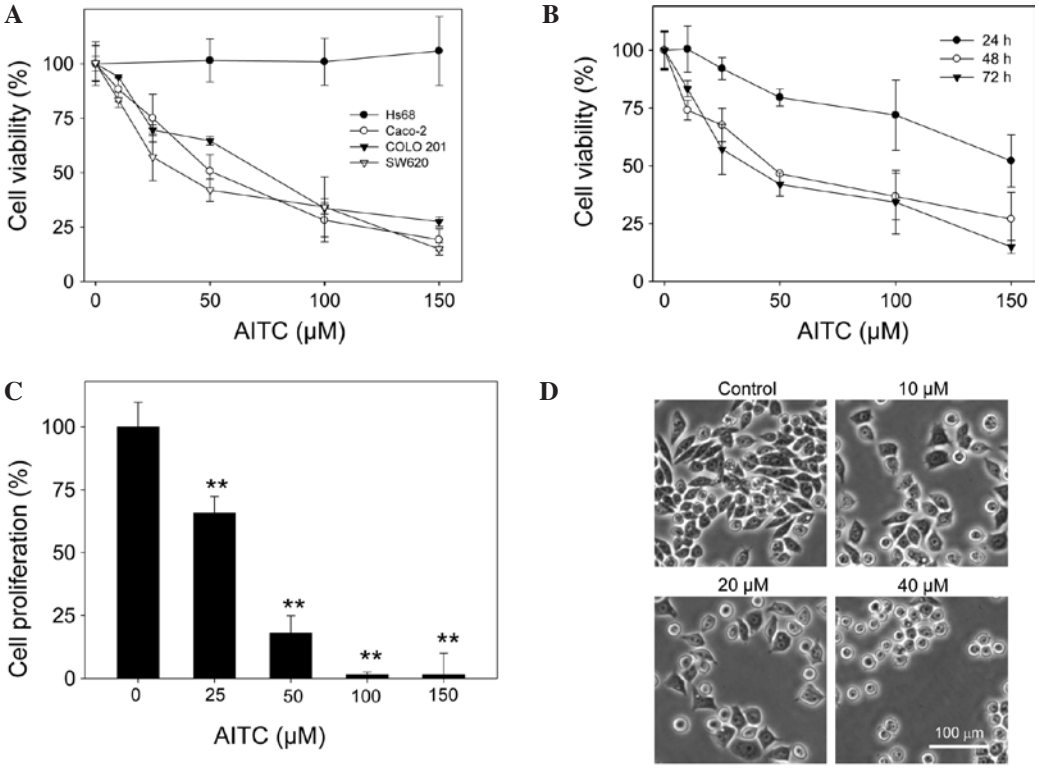

Figure 1. Effects of AITC on the viability and proliferation of various human cell lines. (A) Effects of AITC (72-h treatment) on the viability of Caco-2, COLO 201, SW620 and Hs68 cells as determined by the MTT assay. (B) Dose- and time-dependent effects of AITC on the viability of SW620 cells as determined by the MTT assay. (C) Inhibitory effects of AITC (24-h treatment) on the proliferation of SW620 cells as determined by the BrdU assay. (D) Representative images of SW620 cells exposed to AITC at various concentrations (0, 10, 20 and 40 μM) for 24 h. Cells were observed under a phase contrast microscope. The results are expressed as the mean ± SD of three independent experiments. Statistical differences between the control and treatment groups were determined using the two-tailed Student's t-test. A difference of *P<0.05 or **P<0.01 was considered statistically significant.

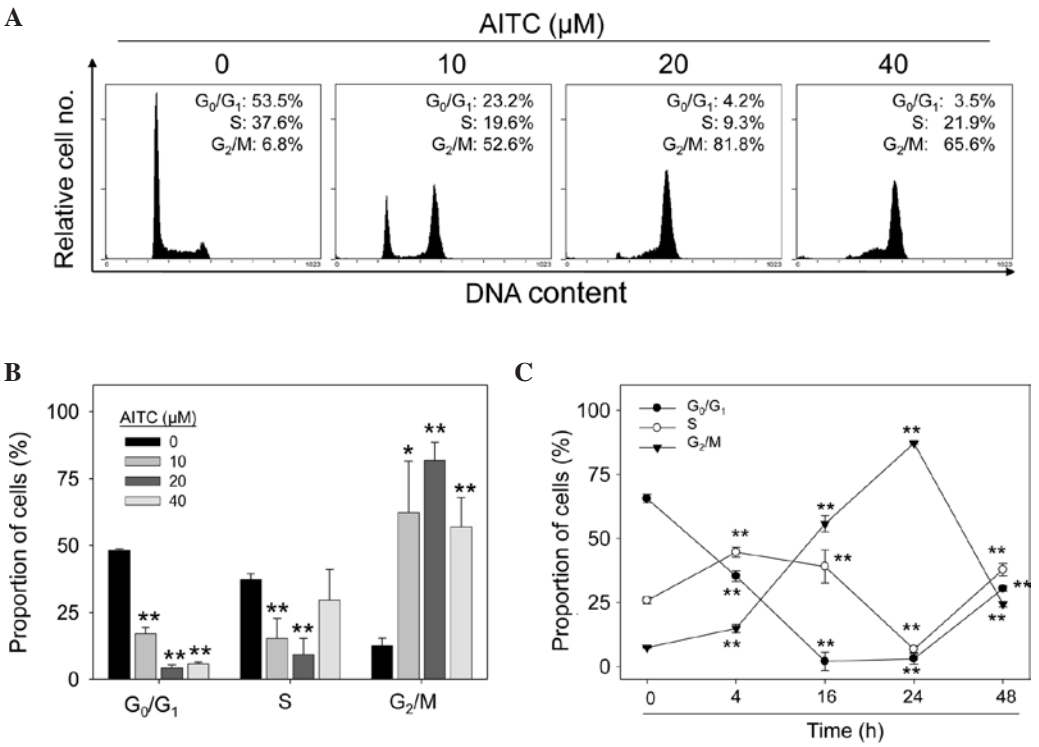

Figure 2. AITC-induced G_2/M arrest in SW620 cells. (A) Cells were treated with AITC at various concentrations (0, 10, 20 and 40 μM) and subjected to flow cytometric analysis of DNA content with propidium iodide staining. (B) Cell cycle analysis of cells exposed to AITC at various concentrations (0, 10, 20 and 40 μM) for 24 h. (C) Time-dependent effects of AITC (20 μM) on cell cycle progression. Results are expressed as the mean ± SD of three independent experiments. Statistical differences between the control and treatment groups were determined by the two-tailed Student's t-test. A difference of *P<0.05 or **P<0.01 was considered statistically significant.

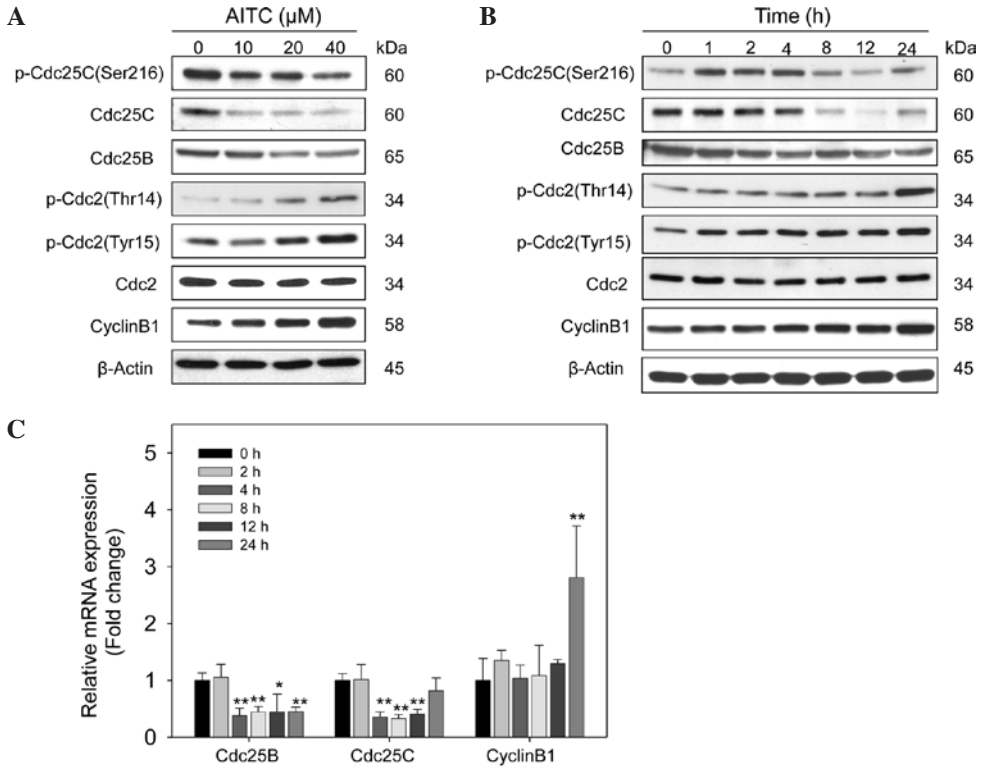

Figure 3. AITC-induced G_2/M arrest in SW620 cells associated with transcriptional and post-translational levels of regulation. Western blot analysis of the expression of p-Cdc25C(Ser216), Cdc25C, Cdc25B, p-Cdc2(Thr14), p-Cdc2(Tyr15), Cdc2 and CyclinB1 proteins after (A) treatment with AITC at various concentrations (10, 20 and 40 μM) for 24 h, and (B) treatment with AITC (20 μM) for varying time periods. (C) Relative mRNA expression of related genes after AITC treatment as determined by real-time quantitative RT-PCR. The expression levels of Cdc25B, Cdc25C and CyclinB1 were normalized by the housekeeping gene GAPDH. Results are expressed as the mean ± SD. Statistical differences between the control and treatment groups were determined using the two-tailed Student's t-test. A difference of *P<0.05 or **P<0.01 was considered statistically significant. At least one independent experiment was performed with similar results.

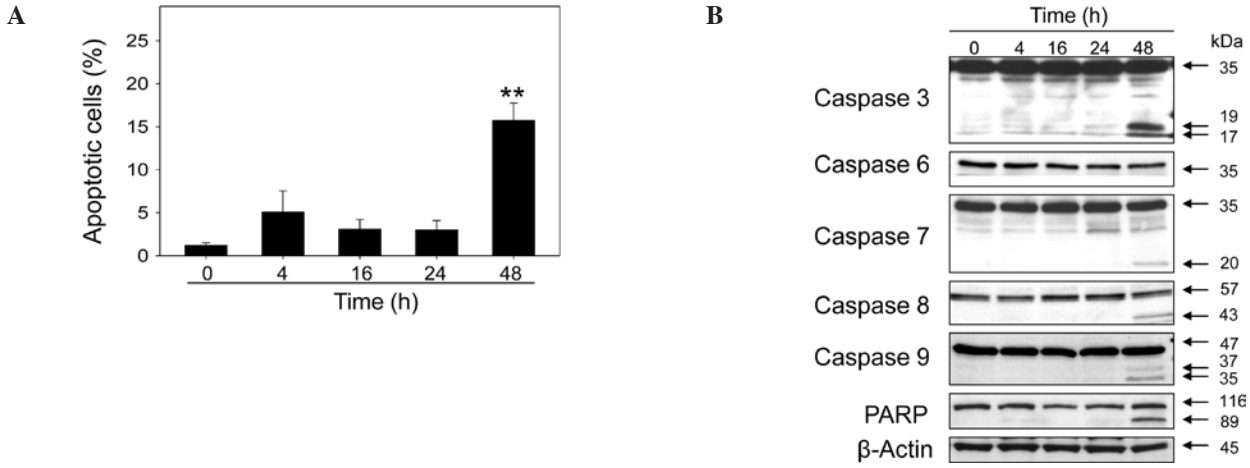

Figure 4. AITC-induced caspase-mediated apoptosis of SW620 cells upon prolonged exposure. (A) Cell apoptosis was induced by AITC (20 μM). The percentage of apoptotic cells was determined by flow cytometric analysis of the cell population at the Sub-G_1 phase. (B) Western blot analysis of the Sub-G_1 expression of caspases (-3, -6, -7, -8 and -9) and PARP after treatment with AITC (20 μM) for varying time periods. Results are expressed as the mean ± SD of three independent experiments. Statistical differences between the control and treatment groups were determined using the two-tailed Student's t-test. A difference of *P<0.05 or **P<0.01 was considered statistically significant.

Cdc25B, Cdc25C and CyclinB1 mRNAs are shown in Fig. 3C. In general, the expression of mRNA was well correlated with the expression of the corresponding protein (Fig. 3B and C). A significant down-regulation of Cdc25B and Cdc25C mRNA was observed 4 h after treatment with 20 μM AITC, and their expression levels remained low (~0.5-fold). By contrast, the up-regulation of CyclinB1 mRNA (~3-fold) was observed after 24 h of treatment (Fig. 3C).

AITC induces caspase-mediated apoptosis after prolonged exposure. Apart from inhibiting cell cycle progression, AITC induced apoptosis in SW620 cells upon prolonged exposure.

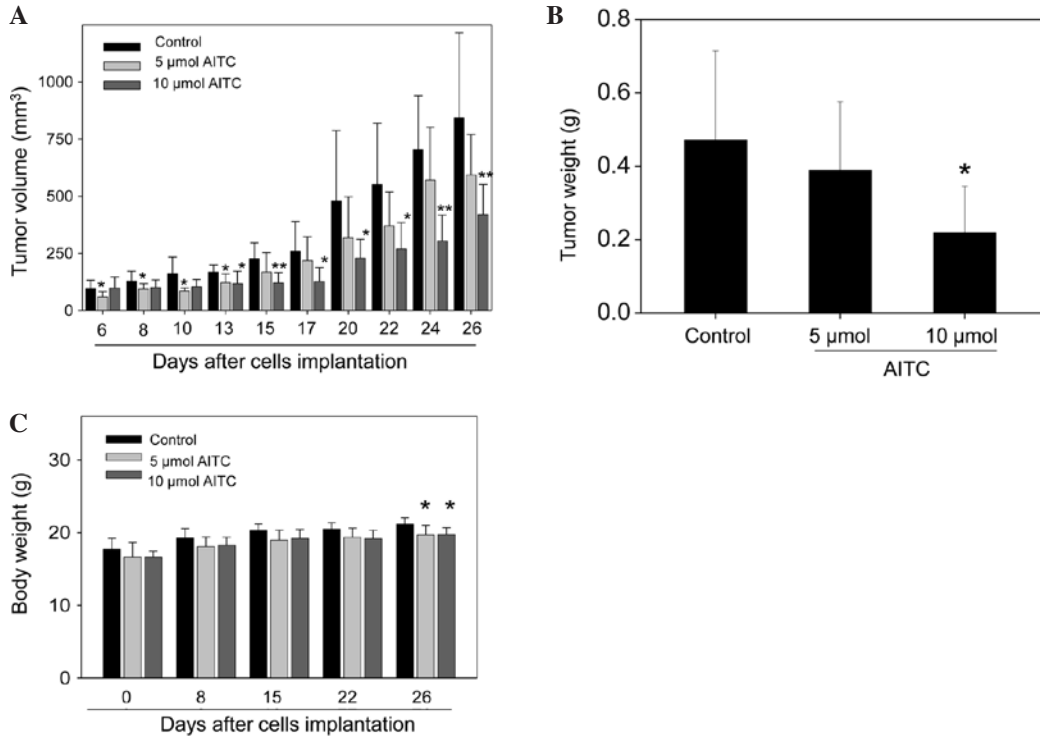

Figure 5. AITC suppression of the growth of SW620 xenografts in nude mice. (A) Changes in the tumor volume in mice receiving various doses of AITC (5 and 10 μmol) during the course of the experiment. (B) Weight of tumors removed from mice receiving varying doses of AITC (5 and 10 μmol) at the termination of the experiment. (C) Changes in the body weight of mice under various treatments during the course of the experiment. Results are expressed as the mean ± SD (n=8 mice/group). Statistical differences between the control and treatment groups were determined using the two-tailed Student's t-test. A difference of $^{*}P<0.05$ or $^{**}P<0.01$ was considered statistically significant.

A significant increase (12.8-fold) in the apoptotic cell population was observed after treatment with 20 μM AITC for 48 h (Fig. 4A). Western blot analysis of key apoptotic proteins in AITC-treated cells revealed a caspase-mediated apoptotic process. As shown in Fig. 4B, AITC induced the cleavage and activation of the initiator caspases (-8 and -9) and the downstream effector caspases (-3 and -7). No cleavage of caspase-6 occurred in SW620 cells exposed to AITC. Proteolytic cleavage of PARP was observed, which served as a key indicator of apoptosis.

AITC suppresses the growth of SW620 xenograft. The *in vivo* antitumor activity of AITC was evaluated in a SW620 xenograft model. Tumor size was measured when palpable tumors appeared on day 6 after cell implantation. As shown in Fig. 5A, a significant suppression of tumor growth was observed in mice treated with 10 μmol AITC throughout the entire experimental period. For example, on day 17 the average tumor volumes of the control and the AITC-treated mice were 261+129 and 127+61 mm^3, respectively. These results reflected a 50% reduction in tumor volume in the treatment group. Similarly, the average tumor volumes and wet tumor weights of the treated mice were ~50% of the control, determined at the termination of the experiment (day 26) (Fig. 5A and B). In order to assess the health of the experimental animals, the body weight of the mice was measured periodically. At the end of the experiment, the body weights of both groups of AITC-treated mice were slightly less (<7%) than those of the control (Fig. 5C). Despite this slight reduction in body weight, all AITC-treated mice appeared healthy and did not show any signs of impaired movement.

Discussion

A high intake of fruits and vegetables has been suggested to provide protective effects against colorectal cancer (2-4). Various dietary phytochemicals have been identified to possess antitumor activities (32). In this study, it was demonstrated that AITC, a constituent of cruciferous vegetables, effectively inhibited the growth and proliferation of human metastatic colorectal adenocarcinoma SW620 cells in a dose- and time-dependent manner (Fig. 1A and B). Flow cytometric analysis of cell cycle progression indicated that the growth-inhibitory effect of AITC against SW620 cells was associated with the induction of G_2/M cell cycle arrest (Fig. 2). This finding is in agreement with other studies showing similar ITCs-induced G_2/M arrest in other cell types (10,12,16-19).

In the control of the cell cycle, activation of the Cdc2/CyclinB protein complex (also known as the mitotic promoting factor) is required for cells to proceed into mitosis (29-31). Prior to mitosis, the catalytic subunit Cdc2 is maintained in an inactive state by phosphorylation on Thr14 and Tyr15 by the action of kinases Wee1 and Myt1. At the G_2/M boundary, dual-specificity phosphatases Cdc25B and Cdc25C remove the Thr14 and Tyr15 phosphorylation on Cdc2, a process that favors the formation of Cdc2/CyclinB. The importance of this passage has been further illustrated by previous studies (33,34). Overexpression of Cdc25B at the mRNA and protein

level was observed in human pancreatic and gastric cancer specimens as compared to their respective normal tissue samples (33,34). In our study, AITC-induced G_2/M arrest was found to be associated with the down-regulation of both the Cdc25B and Cdc25C proteins (Fig. 3A and B). Our findings are consistent with the results of previous studies (16-19,35). However, as the majority of these studies only focused on the post-translational level of regulation, we attempted to extend our investigation further into the transcriptional level of control. The results of quantitative real-time PCR indicated a significant time-dependent down-regulation of Cdc25B and Cdc25C mRNA levels in AITC-treated SW620 cells (Fig. 3C). Without the catalytic action of these two phosphatases, an accumulation of inhibitory phosphorylation on Thr14 and Tyr15 of Cdc2 occurred (Fig. 3A and B), which blocked the G_2/M passage. The importance of transcriptional control in cells arrested at the G_2/M phase was recently reported (35,36). An up-regulation of CyclinB1 at both the mRNA and protein level was also observed in our study (Fig. 3). Such increases may be due to the rise in the number of cells at the G_2/M phase (10,13).

Besides inducing cell cycle arrest, AITC also induced apoptosis in SW620 cells upon prolonged exposure (Fig. 4A). In order to delineate the apoptotic signaling pathway, the expression of key apoptotic proteins in AITC-treated SW620 cells was examined using Western blot analysis. As shown in Fig. 4B, AITC-induced apoptosis was associated with the activation of initiator caspases (-8 and -9) and effector caspases (-3 and -7, but not -6), leading to the cleavage of PARP, which is an indicator of cell apoptosis. Induction of caspase-mediated apoptosis by SFN and PEITC in other cancer cell lines has been reported (9,14,16). Apart from an *in vitro* antitumor effect, our results also suggest that AITC exhibits chemotherapeutic activity *in vivo*. As shown in Fig. 5A, AITC-treatment (10 μmol, 3 times/week) effectively suppressed the growth of SW620 xenografts in nude mice.

In conclusion, our results showed that AITC induced G_2/M arrest in metastatic human colorectal adenocarcinoma SW620 cells through regulation of pivotal regulatory proteins at both the transcriptional and post-translational levels. A prolonged period of AITC exposure triggered caspase-mediated cell apoptosis. On the other hand, AITC exerted minimal toxicity in normal human skin fibroblast Hs68 cells. Besides *in vitro* experiments, an *in vivo* antitumor effect of AITC was demonstrated in an SW620 xenograft study. Taken together, our findings suggest that AITC is a potential candidate for future research in chemoprevention and chemotherapy.

Acknowledgements

This study was supported by the Chinese University of Hong Kong IPMBAB Research Fund and Food Science Research Fund, the Natural Science Foundation of China and Guangdong Province, and the Outstanding Talents Foundation of Jinan University.

References

1. Parkin DM, Bray F, Ferlay J and Pisani P: Global cancer statistics, 2002. CA Cancer J Clin 55: 74-108, 2005.
2. Lin HJ, Probst-Hensch NM, Louie AD, *et al*: Glutathione transferase null genotype, broccoli, and lower prevalence of colorectal adenomas. Cancer Epidemiol Biomarkers Prev 7: 647-652, 1998.
3. Steinmetz KA and Potter JD: Vegetables, fruit, and cancer prevention: a review. J Am Diet Assoc 96: 1027-1039, 1996.
4. Verhoeven DT, Goldbohm RA, van Poppel G, Verhagen H and van den Brandt PA: Epidemiological studies on brassica vegetables and cancer risk. Cancer Epidemiol Biomarkers Prev 5: 733-748, 1996.
5. Fenwick GR, Heaney RK and Mullin WJ: Glucosinolates and their breakdown products in food and food plants. Crit Rev Food Sci Nutr 18: 123-201, 1983.
6. Cheng DL, Hashimoto K and Uda Y: In vitro digestion of sinigrin and glucotropaeolin by single strains of Bifidobacterium and identification of the digestive products. Food Chem Toxicol 42: 351-357, 2004.
7. Elfoul L, Rabot S, Khelifa N, Quinsac A, Duguay A and Rimbault A: Formation of allyl isothiocyanate from sinigrin in the digestive tract of rats monoassociated with a human colonic strain of Bacteroides thetaiotaomicron. FEMS Microbiol Lett 197: 99-103, 2001.
8. Krul C, Humblot C, Philippe C, *et al*: Metabolism of sinigrin (2-propenyl glucosinolate) by the human colonic microflora in a dynamic in vitro large-intestinal model. Carcinogenesis 23: 1009-1016, 2002.
9. Chu WF, Wu DM, Liu W, *et al*: Sulforaphane induces G2-M arrest and apoptosis in high metastasis cell line of salivary gland adenoid cystic carcinoma. Oral Oncol 45: 998-1004, 2009.
10. Gamet-Payrastre L, Li P, Lumeau S, *et al*: Sulforaphane, a naturally occurring isothiocyanate, induces cell cycle arrest and apoptosis in HT29 human colon cancer cells. Cancer Res 60: 1426-1433, 2000.
11. Kuang YF and Chen YH: Induction of apoptosis in a non-small cell human lung cancer cell line by isothiocyanates is associated with P53 and P21. Food Chem Toxicol 42: 1711-1718, 2004.
12. Pappa G, Bartsch H and Gerhauser C: Biphasic modulation of cell proliferation by sulforaphane at physiologically relevant exposure times in a human colon cancer cell line. Mol Nutr Food Res 51: 977-984, 2007.
13. Rose P, Whiteman M, Huang SH, Halliwell B and Ong CN: beta-Phenylethyl isothiocyanate-mediated apoptosis in hepatoma HepG2 cells. Cell Mol Life Sci 60: 1489-1503, 2003.
14. Satyan KS, Swamy N, Dizon DS, Singh R, Granai CO and Brard L: Phenethyl isothiocyanate (PEITC) inhibits growth of ovarian cancer cells by inducing apoptosis: role of caspase and MAPK activation. Gynecol Oncol 103: 261-270, 2006.
15. Singh AV, Xiao D, Lew KL, Dhir R and Singh SV: Sulforaphane induces caspase-mediated apoptosis in cultured PC-3 human prostate cancer cells and retards growth of PC-3 xenografts in vivo. Carcinogenesis 25: 83-90, 2004.
16. Singh SV, Herman-Antosiewicz A, Singh AV, *et al*: Sulforaphane-induced G2/M phase cell cycle arrest involves checkpoint kinase 2-mediated phosphorylation of cell division cycle 25C. J Biol Chem 279: 25813-25822, 2004.
17. Tang L and Zhang Y: Dietary isothiocyanates inhibit the growth of human bladder carcinoma cells. J Nutr 134: 2004-2010, 2004.
18. Xiao D, Johnson CS, Trump DL and Singh SV: Proteasome-mediated degradation of cell division cycle 25C and cyclin-dependent kinase 1 in phenethyl isothiocyanate-induced G2-M-phase cell cycle arrest in PC-3 human prostate cancer cells. Mol Cancer Ther 3: 567-575, 2004.
19. Xiao D, Srivastava SK, Lew KL, *et al*: Allyl isothiocyanate, a constituent of cruciferous vegetables, inhibits proliferation of human prostate cancer cells by causing G2/M arrest and inducing apoptosis. Carcinogenesis 24: 891-897, 2003.
20. Boysen G, Kenney PM, Upadhyaya P, Wang M and Hecht SS: Effects of benzyl isothiocyanate and 2-phenethyl isothiocyanate on benzo[a]pyrene and 4-(methylnitrosamino)-1-(3-pyridyl)-1-butanone metabolism in F-344 rats. Carcinogenesis 24: 517-525, 2003.
21. Nishikawa A, Furukawa F, Uneyama C, *et al*: Chemopreventive effects of phenethyl isothiocyanate on lung and pancreatic tumorigenesis in N-nitrosobis(2-oxopropyl)amine-treated hamsters. Carcinogenesis 17: 1381-1384, 1996.
22. Staretz ME, Koenig LA and Hecht SS: Effects of long term dietary phenethyl isothiocyanate on the microsomal metabolism of 4-(methylnitrosamino)-1-(3-pyridyl)-1-butanone and 4-(methylnitrosamino)-1-(3-pyridyl)-1-butanol in F344 rats. Carcinogenesis 18: 1715-1722, 1997.

23. Srivastava SK, Xiao D, Lew KL, *et al*: Allyl isothiocyanate, a constituent of cruciferous vegetables, inhibits growth of PC-3 human prostate cancer xenografts in vivo. Carcinogenesis 24: 1665-1670, 2003.
24. Chen T and Wong YS: Selenocystine induces S-phase arrest and apoptosis in human breast adenocarcinoma MCF-7 cells by modulating ERK and Akt phosphorylation. J Agric Food Chem 56: 10574-10581, 2008.
25. Chen T, Wong YS, Zheng W and Liu J: Caspase- and p53-dependent apoptosis in breast carcinoma cells induced by a synthetic selenadiazole derivative. Chem Biol Interact 180: 54-60, 2009.
26. Ismail IA, Kang KS, Lee HA, Kim JW and Sohn YK: Genistein-induced neuronal apoptosis and G2/M cell cycle arrest is associated with MDC1 up-regulation and PLK1 down-regulation. Eur J Pharmacol 575: 12-20, 2007.
27. Livak KJ and Schmittgen TD: Analysis of relative gene expression data using real-time quantitative PCR and the 2(-Delta Delta C(T)) method. Methods 25: 402-408, 2001.
28. Kong CK, Lam WS, Chiu LC, Ooi VE, Sun SS and Wong YS: A rice bran polyphenol, cycloartenyl ferulate, elicits apoptosis in human colorectal adenocarcinoma SW480 and sensitizes metastatic SW620 cells to TRAIL-induced apoptosis. Biochem Pharmacol 77: 1487-1496, 2009.
29. Molinari M: Cell cycle checkpoints and their inactivation in human cancer. Cell Prolif 33: 261-274, 2000.
30. Shackelford RE, Kaufmann WK and Paules RS: Oxidative stress and cell cycle checkpoint function. Free Radic Biol Med 28: 1387-1404, 2000.
31. Strausfeld U, Labbe JC, Fesquet D, *et al*: Dephosphorylation and activation of a p34cdc2/cyclin B complex in vitro by human CDC25 protein. Nature 351: 242-245, 1991.
32. Surh YJ: Cancer chemoprevention with dietary phytochemicals. Nat Rev Cancer 3: 768-780, 2003.
33. Guo J, Kleeff J, Li J, *et al*: Expression and functional significance of CDC25B in human pancreatic ductal adenocarcinoma. Oncogene 23: 71-81, 2004.
34. Kudo Y, Yasui W, Ue T, *et al*: Overexpression of cyclin-dependent kinase-activating CDC25B phosphatase in human gastric carcinomas. Jpn J Cancer Res 88: 947-952, 1997.
35. Nigam N, Prasad S, George J and Shukla Y: Lupeol induces p53 and cyclin-B-mediated G2/M arrest and targets apoptosis through activation of caspase in mouse skin. Biochem Biophys Res Commun 381: 253-258, 2009.
36. Prasad S, Nigam N, Kalra N and Shukla Y: Regulation of signaling pathways involved in lupeol induced inhibition of proliferation and induction of apoptosis in human prostate cancer cells. Mol Carcinog 47: 916-924, 2008.